Characterization of Blood Flow Turbulence With Pulsed-Wave and Power Doppler Ultrasound Imaging

Guy Cloutier

Louis Allard

Louis-Gilles Durand

Laboratoire de génie biomédical,
Institut de recherches cliniques
de Montréal,
110 avenue des Pins Ouest,
Montréal, Québec, Canada, H2W 1R7

Blood flow turbulence downstream of a concentric 86 percent area reduction stenosis was characterized using absolute and relative Doppler spectral broadening measurements, relative Doppler velocity fluctuation, and Doppler backscattered power. Bidimensional mappings of each Doppler index were obtained using a 10 MHz pulsed-wave Doppler system. Calf red cells suspended in a saline solution were used to scatter ultrasound and were circulated in an in vitro steady flow loop model. Results showed that the absolute spectral broadening was not a good index of turbulence because it was strongly affected by the deceleration of the jet and by the shear layer between the jet and the recirculation zones. Relative Doppler spectral broadening (absolute broadening divided by the frequency shift), velocity fluctuation, and Doppler power indices provided consistent mapping of the centerline axial variation of turbulence evaluated by hot-film anemometry. The best agreement between the hot-film and Doppler ultrasound methods was however obtained with the Doppler backscattered power. The most consistent bidimensional mapping of the flow characteristics downstream of the stenosis was also observed with the Doppler power index. The relative broadening and the velocity fluctuation produced artifacts in the shear layer and in the recirculation zones. Power Doppler imaging is a new emerging technique that may provide reliable in vivo characterization of blood flow turbulence.

Introduction

Modern real-time ultrasound flow imaging systems combine a gray-scale image of the scanned anatomy with an image produced by the color Doppler and power Doppler modes (Wells, 1994). Conventional pulsed-wave (PW) and continuous-wave (CW) Doppler are used for quantitative in vivo evaluations of the flow characteristics in vessels. The observation of PW and CW Doppler spectral broadening and the mosaic pattern on color Doppler flow images are certainly the most important features attributed to the presence of turbulence in the human circulatory system. The visual inspection of an enlargement of the spectral bandwidth (Taylor et al., 1988; Strandness, Jr. 1990) and the evaluation of spectral broadening indices (Evans et al., 1989) have been used for many years to grade vascular stenoses.

In addition to the presence of turbulence, other factors contributing to the width of the spectrum were reported (Forster, 1977; Jones, 1993; Cloutier et al., 1993). These factors are the intrinsic Doppler spectral broadening that is a function of the Doppler angle (Newhouse et al., 1980), the changes in velocity with space, the changes in velocity with time, and the properties of the spectrum analyzer. Downstream of a stenosis, the broadenings produced by the shear layer (Hutchison, 1993) and flow deceleration (Fish, 1991) probably dominate the broadening associated with turbulence. However, at the centerline where the velocity is fairly constant with radial position, and after flow deceleration, turbulence can be an important factor affecting the broadening of the Doppler spectrum.

The measurement of the temporal fluctuation of the Doppler mean velocity, obtained by using a phase-lock loop frequency tracking method, was proposed to characterize turbulence (Giddens and Khalifa, 1982; Casty and Giddens, 1984; Talukder et al., 1986). Recently, a specially designed cuff containing 5 Doppler probes was used for in vivo mapping of the turbulent velocity fluctuations across the aorta (Nygaard et al., 1994a; 1994b; Kim et al., 1994). Radial variations of the turbulent Reynolds normal stress (RNS) downstream of graded stenoses in pigs (Kim et al., 1994) and bidimensional mapping of RNS downstream of aortic prosthetic valves in humans (Nygaard et al., 1994b) were reported. Limitations of the ultrasonic Doppler derived velocity fluctuations are the limited spatial resolution of the technique, the relatively low frequency response (<500 Hz), and the angle dependence. The difficulty in obtaining the velocity fluctuation in real time and the lack of availability of this index from commercially available ultrasound equipment have probably contributed to its limited clinical use.

The first experimental study showing an increase of the ultrasonic pulse-echo backscattered power in the presence of blood flow disturbance was reported by Shung et al. (1984). Since then, studies by Bascom et al. (1988), Shung et al. (1992), Cloutier and Shung (1993), Bascom et al. (1993), and Cloutier et al. (1995) investigated the effect of turbulence on the Doppler backscattered power. Measurements of the Doppler power were made upstream and downstream of tube constrictions under steady (Bascom et al., 1993) and pulsatile flows (Cloutier et al., 1995). An increase of the power by approximately 3 dB was measured downstream of severe stenoses in those experiments. A power increase of 5.5 dB was found downstream of a grid under pulsatile flow (Cloutier and Shung, 1993).

The objective of the present study was to compare the ability of Doppler spectral broadening measurements (absolute and relative), the relative temporal fluctuation of the Doppler mean velocity, and the Doppler backscattered power in characterizing blood flow turbulence downstream of a severe stenosis under steady flow. Axial centerline measurements at different dis-

Contributed by the Bioengineering Division for publication in the JOURNAL OF BIOMECHANICAL ENGINEERING. Manuscript received by the Bioengineering Division January 4, 1995; revised manuscript received August 10, 1995. Associate Technical Editor: J. M. Tarbell

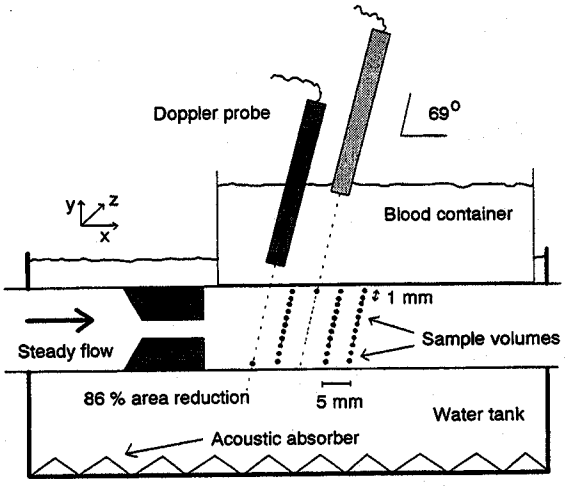

Fig. 1 Schematic representation of the mock flow model used to obtain the bidimensional mapping of the Doppler indices.

tances from the stenosis as well as bidimensional mappings were performed. The Doppler ultrasound indices measured downstream of the stenosis were compared to hot-film anemometry experimental results reproduced from the literature.

Materials and Methods

Experiments were performed in a steady flow model immersed in a water tank, at room temperature. The main flow conduit was a thin-wall heat-shrinkable transparent Kynar tubing having a diameter of 1.27 cm. An acrylic 86 percent area reduction stenosis was positioned inside the Kynar tube as shown in Fig. 1. The length of the stenosis was 6.7 cm and its tapering distance was 1.2 cm (θ = 17 deg). The inlet length of the tube between any curvature and the throat of the stenosis was sufficient to have fully developed laminar flow (d = 50 cm).

A reservoir of 1 liter allowed the filling of the model with blood. Continuous mixing of the solution was performed by a magnetic stirrer. A peristaltic pump (lung-heart pump, Sarns Inc.) circulated the blood at a constant flow rate of 1.8 liter/min. A custom made damping filter was located between the pump and the test section to eliminate the oscillations produced by the rotation of the head of the pump. The flow rate was continuously monitored with a cannulating type flow probe (Carolina Medical Electronics, model SF625) connected to an electromagnetic blood flowmeter (Carolina Medical Electronics, Cliniflow II, model FM701D).

Washed calf red cells suspended in an isotonic saline solution (Celline II™) at a hematocrit of 40 percent were circulated in the flow model. Blood at normal hematocrit instead of any analog fluid was used as the ultrasonic scattering medium because the fluctuation in the concentration of red cells and the hematocrit are known to influence the acoustic backscattering property (Shung et al., 1984; Mo and Cobbold, 1992). Bovine albumin was added to the suspended red cells at a concentration of 0.5 percent to prevent crenation of erythrocytes. At the beginning and the end of each experiment, the hematocrit obtained by micro-centrifugation (Haemofuge, Heraeus Instruments), the temperature, the pH (Sentron, model 1001), and the dynamic viscosity at different shear rates (Brookfield cone-plate viscometer, model LVDVIII-CP-42) were measured. A total of 12 experiments were performed on different days with different blood samples.

Bidimensional Mapping of the Doppler Indices Downstream of the Stenosis. Doppler measurements were performed with a pulsed-wave 10-MHz Doppler system developed at Baylor College of Medicine, Houston, Texas. A pulse-repetition frequency of 39 kHz and a high-pass clutter filter of 100 Hz (−3 dB) were used. The angle between the tube axis and the 3 mm by 3 mm nonfocused Doppler transducer was maintained at 69 deg, as shown in Fig. 1. The transducer was positioned above the tube and at its center in the z direction. Bidimensional mappings of the Doppler derived indices were obtained by moving the transducer axially and radially. The axial and radial resolutions of the images produced with this setup were 5 and 1 mm, respectively. Eleven measurements were performed across the tube for each axial position, as shown in Fig. 1. Data recordings were performed between 0.2 and 10.0 tube diameters (D) downstream of the stenosis with an axial displacement of 0.4 D (5 mm). No post-processing of the images was performed.

For correctly representing the power Doppler images, some parameters needed to be controlled. These are the transmitted power, the size of the sample volume, and the properties of the attenuating medium between the transducer and the location of the sample volume. In the present study, the transmitted power, the sample volume size, and the transmission path length were all kept constant for a given series of measurements. The transducer instead of the position of the gated echoes was moved to maintain a constant sample volume size. The distance between the face of the transducer and the recording sites was then constant, as shown in Fig. 1. Moreover, the transducer was inserted in a blood container laid on the tube to provide the same attenuating properties between the Doppler probe and the location of the sample volume. The attenuation due to the wall of the tube, the thin film of water between the tube and the container, and the bottom of the container made of cellophane was constant for all measurements. Mixing of blood in the containers was performed regularly to keep the solution homogeneous. The size of the sample volume at −3 dB, as determined experimentally with the method described in Cloutier et al. (1995), was approximately 3.3 mm^3. To help the positioning of the sample volumes, a Brüel & Kjaer audio analyzer (model 2012) was used to monitor the Doppler frequency shift.

Centerline Axial Variation of the Doppler Indices and Effect of the Size of the Sample Volume on the Doppler Power. The experimental arrangement shown in Fig. 2 was used to measure specifically, over several experiments, the axial variation of the Doppler indices at the center of the tube. The effect of varying the size of the sample volume on the Doppler power was also tested by moving the transducer upward and by using the second sample volume location. The effect of the size of the sample volume on the other Doppler indices was not tested. Moving the transducer upward resulted in a larger

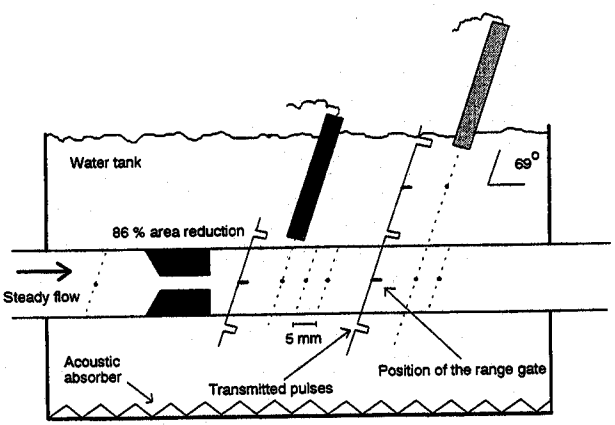

Fig. 2 Experimental setup showing the method used to determine the centerline axial variation of the Doppler indices and the effect of the sample volume size on the Doppler power.

sample volume because of the divergence of the nonfocused ultrasound beam. The theoretical angle of divergence of the transducer in the far field was 3.7 deg (Christensen, 1988).

A first series of measurements was performed by positioning the transducer at a fixed distance near the vessel wall. The range gate control was adjusted to record the backscattered echoes from the center of the tube by maximizing the mean frequency shift measured with the Brüel & Kjaer audio analyzer. At this position, the second and additional sample volumes were located outside the tube. No Doppler signal was detected by those additional gates. In a second series of measurements, the range gate delay was kept unchanged but the transducer was moved upward with a micro-manipulator until the Doppler mean frequency shift matched that recorded previously at the centerline. At this new position, Doppler signals were recorded within the second sample volume delayed with respect to the first one by the pulse repetition interval (25.6 μs). The first, third and other sample volumes were located in the water tank and no Doppler power was attributed to those gated echoes.

With this procedure, two different sample volume sizes were tested. The smaller sample volume had a dimension of 2.9 mm^3 at -3 dB while the larger one had a value of 8.9 mm^3 at -3 dB. Since the transducer was not moved radially for each series of measurements (for a given sample volume size), the possible variation in the attenuation from different media had not to be taken into consideration. Consequently, the Doppler probe was positioned in a water tank to facilitate the experiments. Measurements were performed at 2.2 D before the stenosis and between 0.2 and 10.0 D after the constriction using a transducer axial displacement of 0.4 D.

Data Acquisition and Spectral Analysis. The Doppler in-phase (I) and quadrature (Q) components were amplified by 10 with an amplifier having a flat frequency response between 10 Hz and 30 kHz. The I and Q components, and the flow signal obtained from the electromagnetic flowmeter were digitized for 5 seconds at sampling rates of 39 kHz and 390 Hz, respectively. The gain of the digitizing board (Data Translation, model DT-2821G-SE) was adjusted between 1 and 8 for each acquisition to minimize the quantization error.

The digitized Doppler signals were subdivided into rectangular windows of 2 ms. A similar temporal resolution was used in other Doppler ultrasound studies (Giddens and Khalifa, 1982; Casty and Giddens, 1984). A time interval of 1 ms separated each window from which a Doppler power spectrum was evaluated using autoregressive (AR) modeling and zero padding over 1024 samples. The Yule-Walker equations and the Levinson-Durbin method were used to compute AR spectra (Guo et al., 1993). The optimal number of poles was determined with the "Akaike's information criterion." A total of 4999 spectra was computed and averaged for each recording site within the tube.

Low-pass filtering of the received echoes at 40 kHz and additional filtering attributable to the sample-and-hold circuitry of the Doppler system reduced the bandwidth of the flowmeter. To minimize errors in the power Doppler determination, the frequency response of the audio circuitry of the Doppler system was determined with the Brüel & Kjaer audio analyzer. The mean spectra were then compensated numerically to have a flat bandwidth between 100 Hz and the pulse repetition frequency (PRF) divided by 2 (19.5 kHz), using the method described in Cloutier et al. (1995). A sampling frequency of 39 kHz was used in the compensation procedure.

Computation of the Doppler Indices. The mapping of blood flow turbulence was obtained by computing spectral broadening indices and Doppler power from the mean spectrum, and the relative temporal fluctuation of the Doppler mean velocity from each spectrum. Both absolute and relative Doppler spectral broadening measurements were evaluated. The absolute spectral broadening of the forward component of the mean spectrum was estimated by evaluating the bandwidth at -5 dB (BW_{-5dB}) of the dominant frequency peak.[1] The absolute spectral broadening normalized by the Doppler mean frequency shift (relative spectral broadening) was also tested.

In experimental studies by Forster (1977) and Garbini et al. (1982), the turbulence intensity measured with hot-film anemometry correlated well with that estimated by the following relative Doppler spectral broadening index I:

$$I = \sqrt{\left(\frac{\sigma}{\mu}\right)^2 - \left(\frac{\sigma}{\mu}\right)_0^2} \cos\theta \tag{1}$$

where σ and μ are the standard deviation and mean frequency shift of the Doppler spectrum, and θ is the angle between the ultrasonic beam and flow direction. The term $(\sigma/\mu)_0$ in Eq. (1) denoted the intrinsic broadening which is the relative broadening in laminar flow with no velocity gradients within the Doppler sample volume. Since this term is constant for a given experimental arrangement and small compared to the relative broadening associated with turbulence (Cloutier et al., 1993), Eq. (1) can be simplified as follow:

$$I \approx \frac{\sigma}{\mu} \cos\theta. \tag{2}$$

In the present study, the relative spectral broadening (RSB) was computed by:

$$\text{RSB} = \frac{BW_{-5dB}}{f_d} \cos\theta \tag{3}$$

where f_d is the Doppler mean frequency shift of the forward flow components evaluated within the bandwidth at -5 dB, which was estimated by using:

$$f_d = \frac{\sum_{f_k=-BW}^{BW} f_k P(f_k)}{\sum_{f_k=-BW}^{BW} P(f_k)} \tag{4}$$

where $\pm BW$ are the higher and lower frequencies of the -5 dB bandwidth. The mean frequency was computed within $\pm BW$ to eliminate the bias attributable to the noisy frequency components of the spectrum. This method was particularly effective for spectra computed using the sample volume of 8.9 mm^3 since the signal-to-noise ratio of those spectra was reduced.

The following equation was used to compute the mean power P of the forward and reverse components of the mean spectrum:

$$P = \frac{1}{N} \sum_{f_k=-PRF/2}^{+PRF/2} P(f_k), \tag{5}$$

where $P(f_k)$ represents the power in a bandwidth $\Delta f = 38$ Hz (39 kHz/1024) centered at the frequency f_k, and $N = 1024$ is the number of samples between $\pm PRF/2$. Equation (5) was used to map, using the experimental arrangement of Fig. 1, the variation of the Doppler backscattered power downstream of the stenosis. The downstream centerline axial values of the Doppler power, obtained by using the model of Fig. 2, were normalized by the power measured before the stenosis and expressed as a power ratio. This procedure was used to eliminate the variance of the results attributable to changes in blood echogenicity from one sample to the other.

The relative velocity fluctuation was computed by assuming that the instantaneous blood velocity at a fixed point of the tube was the sum of a mean velocity $U(t)$ and a fluctuating or

[1] Two peaks were found for spectra recorded in the boundary layer between the jet and the recirculation zone. For this specific situation, only the -5 dB bandwidth of the dominant peak was used.

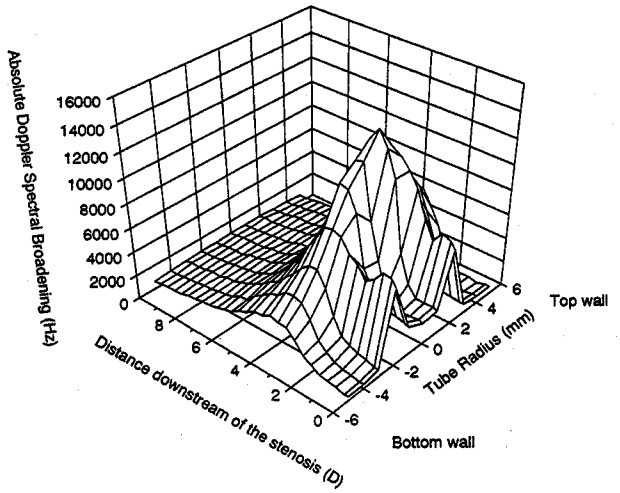

Fig. 3 Example of a bidimensional mapping of the absolute Doppler spectral broadening downstream of the 86 percent area reduction stenosis.

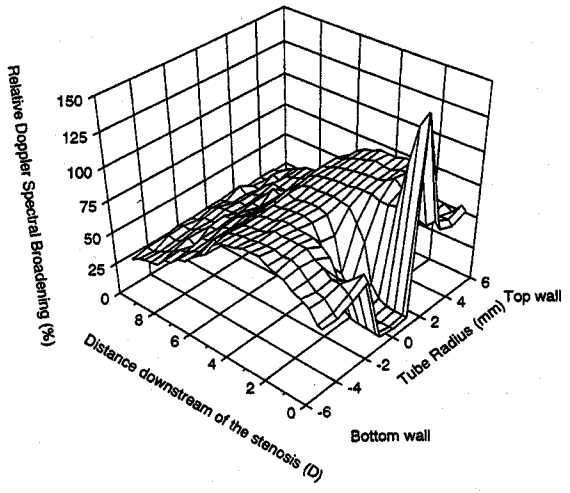

Fig. 4 Example of a bidimensional mapping of the relative Doppler spectral broadening downstream of the 86 percent area reduction stenosis.

turbulent velocity $u'(t)$. The relative velocity fluctuation RVF was estimated by:

$$\text{RVF} = \frac{\text{RMS}[u']}{\langle U \rangle} = \frac{\text{RMS}[f_d']}{\langle f_d \cos(\theta) \rangle} \quad (6)$$

where RMS is the root-mean-square mathematical operation and $\langle\rangle$ the time averaging operation. The mean frequency shift f_d of the forward flow component was estimated from each spectrum computed over a time interval of 2 ms, using Eq. (4). The fluctuating components f_d' were extracted by removing the time-averaged value ($\langle f_d \cos(\theta) \rangle$) from each computed value of f_d. The parameter $\langle f_d \cos(\theta) \rangle$ was obtained by averaging data over the interval of 5 seconds ($n = 4999$). As suggested by Casty and Giddens (1984), the angular correction was performed only for the mean velocity $\langle U \rangle$. No correction was done for the fluctuating velocity components u' because turbulence is a three-dimensional phenomenon.

Results

All results are expressed in term of mean ± one standard deviation (SD). The mean flow was computed from the digitized data for each recording site. The mean value averaged over all experiments was 1.78 ± 0.02 l/min. Assuming Poiseuille flow before the stenosis, the spatial mean shear rate was 98.3 s^{-1}. The dynamic viscosity of blood was determined for all blood samples, at a shear rate of 98.3 s^{-1}, and was 5.2 ± 0.3 mPa·s. The hematocrit, pH, temperature, and upstream Reynolds number were 40.0 ± 0.4%, 7.1 ± 0.1, 22.9 ± 0.8°C, and 633 ± 42, respectively.

Bidimensional Mapping of the Doppler Indices Downstream of the Stenosis. Figures 3 to 6 show examples, obtained from one experiment, of the bidimensional distribution of the absolute and relative Doppler spectral broadening, relative fluctuation of the mean velocity, and Doppler backscattered power, respectively. As seen in Fig. 3, the absolute broadening was low in the recirculation zones and in the jet close to the stenosis, and maximal at the center of the tube 4.3 D after the stenosis. The boundary layer between the jet and the recirculation zones also increased the absolute broadening of the mean spectra. The relative spectral broadening (see Fig. 4) was minimum in the jet, at the center of the tube, and showed high unstable values in the boundary layer. A plateau was observed all across the tube diameter around 5.3 D and the relative broadening dropped further downstream. As seen in Fig. 5, the rela-

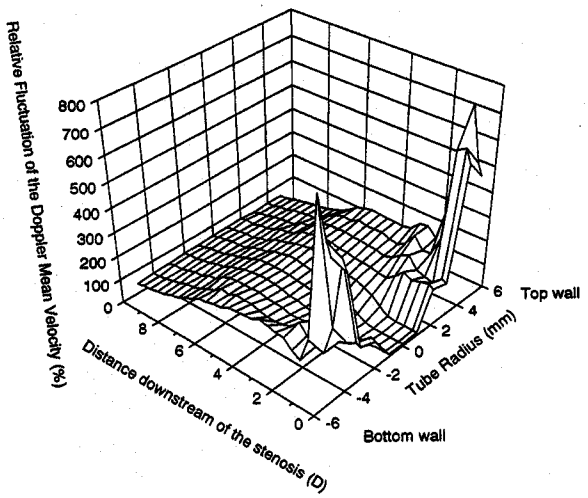

Fig. 5 Example of a bidimensional mapping of the relative fluctuation of the Doppler mean velocity downstream of the 86 percent area reduction stenosis.

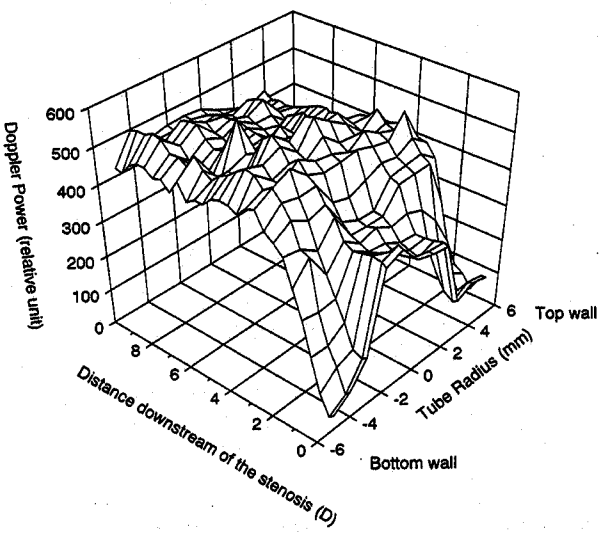

Fig. 6 Example of a bidimensional mapping of the Doppler power downstream of the 86 percent area reduction stenosis.

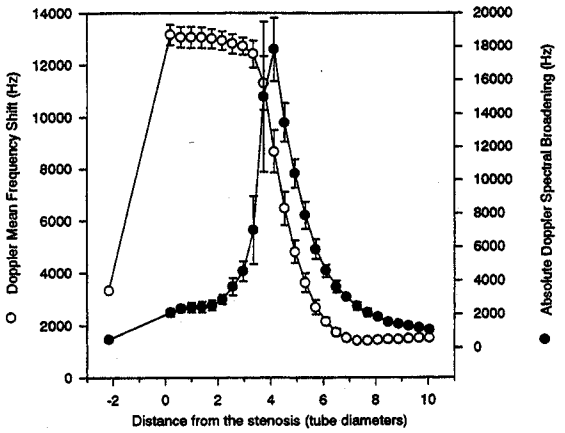

Fig. 7 Centerline axial variation of the Doppler mean frequency shift f_d and absolute spectral broadening. Results are expressed in terms of mean ± one standard deviation (N = 9 experiments).

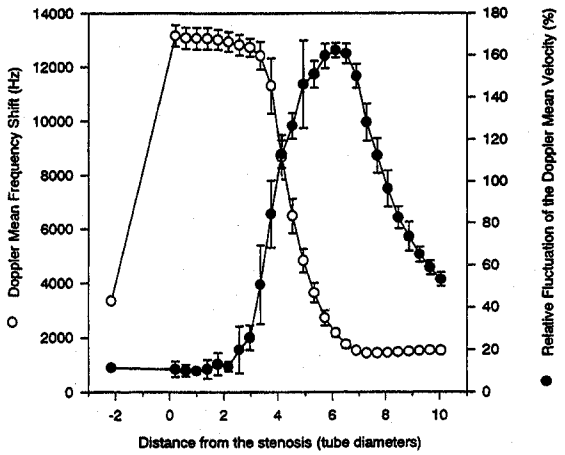

Fig. 9 Centerline axial variation of the Doppler mean frequency shift f_d and relative fluctuation in time of the Doppler mean velocity. Results are expressed in terms of mean ± one standard deviation (N = 9 experiments).

tive fluctuations of the velocity depicted some instabilities in the recirculation zones. At the center of the tube, the fluctuation was low in the jet, increased downstream, and returned to a low value further downstream. The Doppler backscattered power showed similar variations at the center of the tube (see Fig. 6). However, the reduction of the power after the maximum was lower than that observed for the velocity fluctuations or the relative spectral broadening. The lowest power was observed in the recirculation zones.

Centerline Axial Variations of the Doppler Indices. To better visualize the axial variation and the reproducibility of the indices, the measurements were repeated over 9 experiments at the center of the tube. The variation of the absolute Doppler spectral broadening is presented in Fig. 7. The broadening slightly increased in the high velocity jet (between 0.2 and 3.4 D), increased rapidly after that to reach a maximum at 4.1 D, and then decreased further downstream. The maximum broadening occurred in the region corresponding to the rapid deceleration of the velocity jet, as shown by the Doppler mean frequency shift curve of Fig. 7. The relative spectral broadening depicted a different axial variation downstream of the stenosis (see Fig. 8). Moreover, the relative broadening peaked farther downstream at 5.7 D.

As shown in Fig. 9, a relative velocity fluctuation of approximately 11 percent was measured upstream, and downstream of the stenosis between 0.2 and 2.2 D. The fluctuation increased after 2.2 D to reach a maximum at 6.1 D. The velocity fluctuation dropped from 162 to 53 percent between 6.1 and 10.0 D. At 10.0 D, the fluctuation was higher than that measured upstream of the stenosis, under laminar flow. The maximal velocity fluctuation occurred toward the end of the flow deceleration. The variation of the Doppler backscattered power as a function of the axial position is presented in Fig. 10. For a sample volume size of 2.9 mm^3 (black circles), the power ratio was constant in the jet (≈1.15) and slightly higher than that measured upstream of the constriction. The ratio increased during the deceleration of the jet to reach a maximum at 6.9 D, where the flow had stopped to decelerate. A maximal power increase of 85 percent (2.7 dB) was measured. The power ratio dropped further downstream and, at 10.0 D, it was 64 percent higher than that observed before the stenosis.

Effect of the Size of the Sample Volume on the Doppler Power Ratio. To verify any possible effect of the size of the sample volume, the measurements were repeated over 4 experiments using a sample volume of 8.9 instead of 2.9 mm^3. Because the ultrasonic beam intercepted the acrylic stenosis for measurements performed at 0.2 D, this recording site was eliminated from

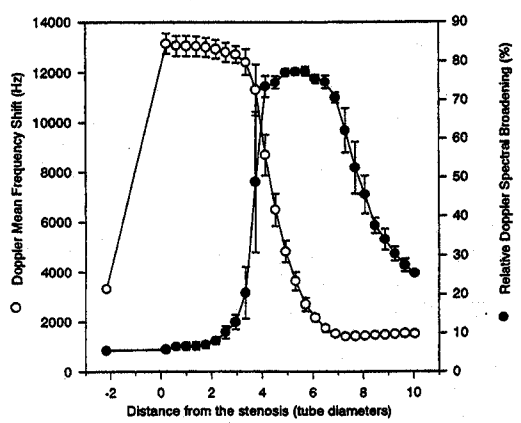

Fig. 8 Centerline axial variation of the Doppler mean frequency shift f_d and relative spectral broadening. Results are expressed in terms of mean ± one standard deviation (N = 9 experiments).

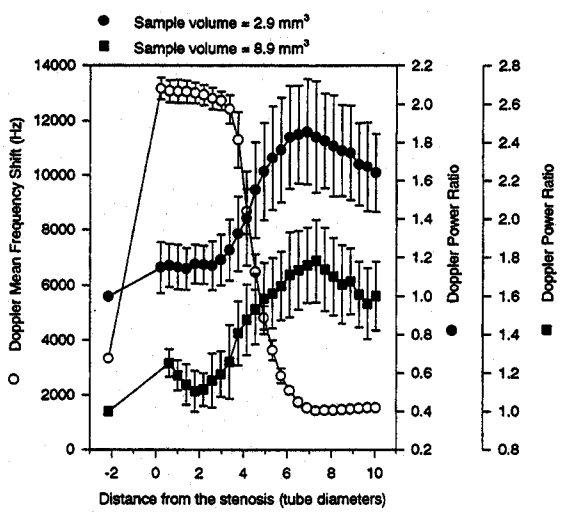

Fig. 10 Centerline axial variation of the Doppler mean frequency shift f_d and power ratios for sample volume sizes of 2.9 mm^3 (black circles) and 8.9 mm^3 (black squares). Results are expressed in terms of mean ± one standard deviation. Doppler measurements were repeated over 9 experiments for the sample volume of 2.9 mm^3 and over 4 experiments for the volume size of 8.9 mm^3.

the results. As seen in Fig. 10, the enlargement of the sample volume had few effect on the Doppler power ratio. The only difference was observed close to the exit of the stenosis. Instead of having a plateau, the power ratios varied between 1.10 and 1.25 for measurements between 0.6 and 2.6 D.

Discussion

Two important reasons prompted us to study the relationship between Doppler ultrasound indices and the flow disturbance produced by a severe stenosis, under steady flow. First, the fact that the flow dynamics downstream of a stenosis was experimentally investigated and described in detail by many authors (Kim and Corcoran, 1974; Cassanova and Giddens, 1978; Young, 1979; Yongchareon and Young, 1979; Ahmed and Giddens, 1983; Jones, 1985) is certainly the main reason because it provided us established references to compare the results obtained with Doppler ultrasound. Secondly, the presence of several and well documented flow conditions, i.e., a high velocity laminar jet, regions of flow separation, recirculation zones characterized by large permanent laminar vortices, reattachment points, vortex shedding before the breaking of the jet, turbulence, and a relaminarization zone, allowed us to test the effects of these flow conditions on the Doppler indices.

Hot-Film and Laser Doppler Turbulence Measurements Downstream of Severe Stenoses. Measurements of the intensity of turbulence produced downstream of severe axisymmetric stenoses were reported using hot-film (Kim and Corcoran, 1974; Cassanova and Giddens, 1978; Yongchareon and Young, 1979; Jones, 1985) and laser Doppler anemometers (Ahmed and Giddens, 1983). Cassanova and Giddens (1978) and Yongchareon and Young (1979) showed that turbulence is first developed near the reattachment points, close to the wall, in the region of the shear layer bounding the jet. In the center of the jet is a region of low intensity fluctuations that remains essentially laminar until turbulence from the shear layer diffuses into it. At this point, the entire flow cross-section has become turbulent. Generally, when turbulence occurs, the jet radius remains fairly constant with axial distance up to the position at which turbulence begins (Jones, 1985).

A very exhaustive study (Yongchareon and Young, 1979) demonstrated the strong influence of the upstream Re on the propagation of turbulence in the shear layer. For a 89 percent area reduction stenosis modeled in a 19.05 mm diameter tube, the maximal turbulence intensity in the shear layer was detected at 12 D for Re between 280 and 450, at 6 D for Re = 633, and at 2 D for Re = 800. Centerline axial measurements of the turbulence intensity as a function of the upstream Re, severity and shape of the stenosis, roughness of the constriction, and vibrations were performed by Jones (1985). The effect of Re on the centerline turbulence intensity was also studied by Ahmed and Giddens (1983). It was found that the more severe the constriction and the higher the Re, the closer the peak is to the constriction. The reattachment length as a function of the shape, severity of the stenosis, and upstream Re was investigated by Young and Tsai (1973), Young (1979), and Chahed et al. (1991). The size of the recirculation zone increased for more severe stenoses while the reattachment length decreased with an increase in Re.

Reproduction of the Results by Jones (1985). Experimental results obtained for flow conditions close to that used in the present study are reproduced here from Jones (1985). Centerline axial measurements of the time-averaged velocity and turbulence intensity were measured using hot-film anemometry downstream of concentric 56 to 89 percent area reduction stenoses at upstream Re between 352 and 1438. As seen in Fig. 11 for 89 and 83 percent area reduction stenoses, and an upstream Re of 662, the relative turbulence intensity increased downstream of the narrowing to reach a maximum and then decreased. The position of the peaks of the relative turbulence intensity occurred near the end of the flow deceleration for both stenoses. For the 89 percent stenosis, the peak was detected at 6.3 D while it was found around 8.0 D for the 83 percent constriction. By linear extrapolation, the peak would be expected around 7.1 D for a 86 percent stenosis. In addition, at Re = 633 instead of 662, the relative turbulence intensity would occur slightly beyond 7.1 D based on the experimental results of Jones (1985).

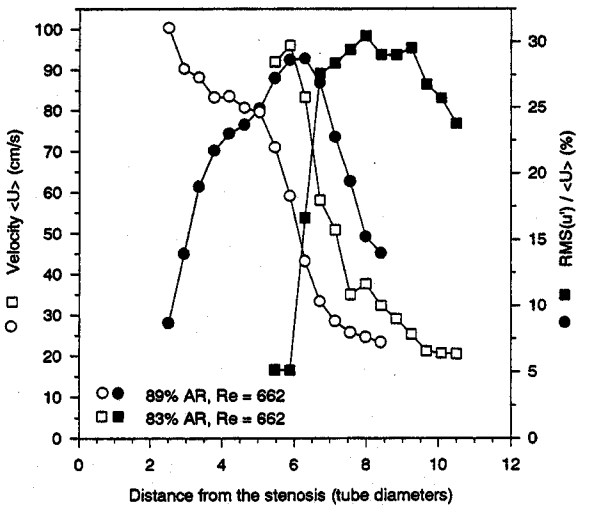

Fig. 11 Centerline axial variation of the time-averaged velocity measured with the hot-film probe ($\langle U \rangle$) and relative turbulence intensity (RMS $[u']/\langle U \rangle$) downstream of 89 and 83 percent area reduction (AR) concentric stenoses. Experimental data were collected in water under steady flow with hot-film anemometry, and were reproduced with permission from Figs. 25, 26, 37, and 38 of Jones (1985).

In the present study, the distances from the stenosis at which any of the four Doppler indices peaked were all smaller than 6.9 D. Since many factors including the shape and length of the stenosis, possible vibration of the flow loop model, the type of fluid, and possible differences in background noise conditions differed between our study and the study of Jones (1985), the comparison of the position of the relative turbulence intensity peak with the peak of the Doppler indices must be done with caution.

Mapping of the Absolute and Relative Doppler Spectral Broadening. As it was demonstrated previously by Hutchison (1993), the present study confirmed the usefulness of the absolute Doppler spectral broadening for detecting the boundary region between the jet and the recirculation zones (see Fig. 3). Although the absolute Doppler spectral broadening is used in clinical practice to qualitatively predict the presence of flow disturbance, it is now well accepted that this index is not reliable to detect blood flow turbulence. For instance, too many instrumental and flow related parameters can influence the bandwidth of the Doppler spectrum (Forster, 1977; Jones, 1993). It was shown in the present study that rapid flow deceleration strongly influenced the bandwidth of the spectra for measurements performed downstream of a severe stenosis. In the region of suspected maximal relative turbulence intensity, near the reattachment point and after the breaking of the jet (around 7 D based on the Doppler mean frequency shift curve), the broadening was small as shown in Figs. 3 and 7.

The relative Doppler spectral broadening was proposed as a quantitative measurement of turbulence in the absence of velocity gradients within the Doppler sample volume (Forster, 1977; Garbini et al., 1982). As shown in Fig. 4, the relative broadening was abnormally high in the shear layer close to the stenosis and in the recirculation zones. The presence of a velocity gradi-

ent in the shear layer and errors in the estimate of the frequency shift, due to a wrong prediction of the Doppler angle in the recirculation regions, may explain these artifacts. As shown in Fig. 8, the relative bandwidth peaked at 5.7 D well before the position predicted by hot-film anemometry. The difference between both results is believed to be explained by the increase of the bandwidth of the Doppler spectrum due to the deceleration of the jet (velocity gradients within the sample volume).

Mapping of the Doppler Mean Velocity Fluctuation. The characterization of the centerline velocity fluctuations shown in Fig. 9 probably provided a realistic distribution of the turbulence intensity downstream of the stenosis. The peak of the relative fluctuation of the Doppler mean velocity occurred at 6.1 D near the end of the flow deceleration. Although the Doppler mean velocity fluctuation provided good results in the centerline of the tube, the instability of this index in the recirculation zones is an important limitation (see Fig. 5). As mentioned previously, drawbacks associated with this index are the limited spatial resolution of the Doppler technique, the relatively low frequency response (<500 Hz), and the angle dependence. It seems from our results that the angle dependence is an important problem. The variation of the angle between the ultrasound beam and the direction of the flow, in the recirculation zones, reduced the accuracy of the Doppler frequency shift estimate and then the stability of the index.

The relative turbulence intensity presented in Fig. 11 barely exceeded 30 percent in the centerline of the tube for both stenoses. In the present study, a value as high as 162 percent was found downstream of the stenosis and a relative velocity fluctuation of 11 percent was measured upstream of the stenosis, under laminar flow (see Fig. 9). In the study by Casty and Giddens (1984), the relative velocity fluctuation measured with Doppler ultrasound under laminar flow conditions was approximately 4 percent. The reasons for the non-zero values under laminar flow and the unexpected high values under turbulent flow are unknown. Velocity-independent instrument noise (Casty and Giddens, 1984), the relatively large size of the sample volume compared to hot-film anemometry, and the limited efficiency of the damping filter used to obtain steady flow may all have contributed.

Mapping of the Doppler Backscattered Power. Measurements of centerline axial variations of the Doppler backscattered power downstream of severe stenoses were reported in other studies (Bascom et al., 1993; Cloutier et al., 1995). In the steady flow experiment performed by Bascom et al. (1993), a power increase by approximately 50 percent was found between 6 and 10 D downstream of an asymmetrical 70 percent area reduction stenosis. Under physiological pulsatile flow, increases in Doppler power ranging approximately between 50 and 100 percent were found 10 D downstream of 75 to 91 percent area reduction stenoses (Cloutier et al., 1995). Similar results were reported in the present study in Fig. 10. For instance, the maximal power increase detected 6.9 D downstream of the 86 percent area reduction constriction was 85 percent. From all Doppler indices tested, the backscattered power provided the best agreement with the hot-film anemometry results. Nevertheless, further results correlating the Doppler power with hot-film anemometry measurements will be needed to better understand the mechanisms involved in the backscattering of Doppler ultrasound from blood under turbulent flow.

From all indices tested, the Doppler power provided the most consistent bidimensional mapping of the flow characteristics downstream of the stenosis. The variability of this index between experiments is, however, its major drawback. The need for averaging the power over several spectra (few seconds) is another limitation. As seen in Fig. 6, the Doppler power was minimum in the recirculation zones, partially because of the effect of the wall filter. The power was higher in the laminar jet and maximal all over the cross-section of the tube after the breaking of the jet. In comparison with the other indices, no artifact was found in the shear layer and in the recirculation zones. It can be suggested from the results of this study that unsteady turbulent eddies may have a stronger effect on the Doppler power than larger permanent vortices since the power was low in the recirculation zones. The relationship between the size of the eddies and the Doppler power is unknown. Further studies will also be needed to elucidate this aspect.

Conclusion

From the four Doppler derived indices tested, the relative Doppler spectral broadening, the velocity fluctuation, and the Doppler power provided consistent estimates of the centerline axial variation of turbulence downstream of the 86 percent area reduction stenosis. The Doppler power was, however, the index providing the best results for detecting the position of the maximum turbulence intensity determined by hot-film anemometry. The most consistent bidimensional mapping of the flow characteristics downstream of the stenosis was also obtained with the power Doppler index. This index provided an efficient detection of the recirculation zones. Absolute Doppler spectral broadening was shown to be inefficient to characterize turbulence but performed well in detecting the boundary layer between the jet and the recirculation zones. The observed limitations of the velocity fluctuation was its instability in the recirculation zones and the abnormally high values compared to hot-film anemometry, while that of the relative spectral broadening was its inconsistency in the shear layer, close to the stenosis, and in the recirculation zones. The Doppler power showed a considerable variability between experiments. The fact that power Doppler ultrasound imaging is available commercially is certainly a major advantage of this index.

Acknowledgment

This work was supported by the Medical Research Council of Canada (#MA-11740) and the Heart and Stroke Foundation of Quebec, and by a research scholarship from the Fonds de la Recherche en Santé du Québec. The authors gratefully acknowledge Dr. Steven A. Jones of the Department of Biomedical Engineering, Johns Hopkins University, for generously providing the data reproduced in Fig. 11. Acknowledgments are also addressed to Drs. Guy Dumas and Jean Lemay of the Department of Mechanical Engineering, Laval University, for helpful discussions.

References

Ahmed, S. A., and Giddens, D. P., 1983, "Flow Disturbance Measurements through a Constricted Tube at Moderate Reynolds Numbers," *J. Biomechanics*, Vol. 16(12), pp. 955–963.

Bascom, P. A. J., Cobbold, R. S. C., Routh, H. F., and Johnston, K. W., 1993, "On the Doppler Signal from a Steady Flow Asymmetrical Stenosis Model: Effects of Turbulence," *Ultrasound Med Biol*, Vol. 19(3), pp. 197–210.

Bascom, P. A. J., Routh, H. F., and Cobbold, R. S. C., 1988, "Interpretation of Power Changes in Doppler Signals from Human Blood - In Vitro Studies," *Ultrasonics Symposium*, Vol. 2, pp. 985–988.

Cassanova, R. A., and Giddens, D. P., 1978, "Disorder Distal to Modeled Stenoses in Steady and Pulsatile Flow," *J Biomechanics*, Vol. 11, pp. 441–453.

Casty, M., and Giddens, D. P., 1984, "25 + 1 Channel Pulsed Ultrasound Doppler Velocity Meter for Quantitative Flow Measurements and Turbulence Analysis," *Ultrasound Med Biol*, Vol. 10(2), pp. 161–172.

Chahed, N., Péronneau, P., Delouche, A., and Diebold, B., 1991, "Velocity Profiles and Streamlines of a Revolution Poststenotic Flow," *Biorheology*, Vol. 28, pp. 383–400.

Christensen, D. A., 1988, "*Ultrasonic Bioinstrumentation*, Wiley, New York, Chichester, Brisbane, Toronto, Singapore.

Cloutier, G., Allard, L., and Durand, L. G., 1995, "Changes in Ultrasonic Doppler Backscattered Power Downstream of Concentric and Eccentric Stenoses Under Pulsatile Flow," *Ultrasound Med Biol*, Vol. 21, pp. 59–70.

Cloutier, G., and Shung, K. K., 1993, "Cyclic Variation of the Power of Ultrasonic Doppler Signals Backscattered by Polystyrene Microspheres and Porcine Erythrocyte Suspensions," *IEEE Trans Biomed Eng*, Vol. 40(9), pp. 953–962.

Cloutier, G., Shung, K. K., and Durand, L. G., 1993, "Experimental Evaluation of Intrinsic and Nonstationary Ultrasonic Doppler Spectral Broadening in Steady and Pulsatile Flow Loop Models," *IEEE Trans Ultrason Ferroelec Freq Cont,* Vol. 40(6), pp. 786–795.

Evans, D. H., McDicken, W. N., Skidmore, R., and Woodcock, J. P., 1989, *Doppler Ultrasound. Physics, Instrumentation, and Clinical Applications,* Wiley, Chichester, New York, Brisbane, Toronto, Singapore.

Fish, P. J., 1991, "Nonstationarity Broadening in Pulsed Doppler Spectrum Measurements," *Ultrasound Med Biol,* Vol. 17(2), pp. 147–155.

Forster, F. K., 1977, "The Applications and Limitations of Doppler Spectral Broadening Measurements for the Detection of Cardiovascular Disorders," *Ultrasound Med,* Vol. 33, pp. 1223–1226.

Garbini, J. L., Forster, F. K., and Jorgensen, J. E., 1982, "Measurement of Fluid Turbulence Based on Pulsed Ultrasound Techniques. Part 2. Experimental Investigation," *J Fluid Mech,* Vol. 118, pp. 471–505.

Giddens, D. P. and Khalifa, A. M. A., 1982, "Turbulence Measurements with Pulsed Doppler Ultrasound Employing a Frequency Tracking Method," *Ultrasound Med Biol,* Vol. 8(4), pp. 427–437.

Guo, Z., Durand, L. G., Allard, L., Cloutier, G., Lee, H. C., and Langlois, Y. E., 1993, "Cardiac Doppler Blood Flow Signal Analysis. Part II: Time-Frequency Representation Based on Autoregressive Modelling," *Med Biol Eng Comput,* Vol. 31, pp. 242–248.

Hutchison, K. J., 1993, "Doppler Ultrasound Spectral Shape in the Poststenotic Velocity Field," *Ultrasound Med Biol,* Vol. 19(8), pp. 649–659.

Jones, S. A., 1985, "A Study of Turbulent Flow Downstream of a Constriction in a Cylindrical Tube at Low Reynolds Numbers with Emphasis on Frequency Correlations," University of California, San Diego, Ph.D. thesis.

Jones, S. A., 1993, "Fundamental Sources of Error and Spectral Broadening in Doppler Ultrasound Signals," *CRC Critical Reviews Biomedical Engineering,* Vol. 21(5), pp. 399–483.

Kim, B. M., and Corcoran, W. H., 1974, "Experimental Measurements of Turbulence Spectra Distal to Stenoses," *J Biomechanics,* Vol. 7, pp. 335–342.

Kim, W. Y., Pedersen, E. M., Nygaard, H., Somod, L., and Hasenkam, J. M., 1994, "Studies by Pulsed Doppler Ultrasonography of Velocity Fields Downstream of Graded Stenoses on the Abdominal Aorta in Pigs," *J Vasc Surg,* Vol. 19, pp. 414–425.

Mo, L. Y. L., and Cobbold, R. S. C., 1992, "A Unified Approach to Modeling the Backscattered Doppler Ultrasound from Blood," *IEEE Trans Biomed Eng,* Vol. 39(5), pp. 450–461.

Newhouse, V. L., Furgason, E. S., Johnson, G. F., and Wolf, D. A., 1980, "The Dependence of Ultrasound Doppler Bandwidth on Beam Geometry," *IEEE Trans Sonics Ultra,* Vol. 27(2), pp. 50–59.

Nygaard, H., Hasenkam, J. M., Pedersen, E. M., Kim, W. Y., and Paulsen, P. K., 1994a, "A New Perivascular Multi-Element Pulsed Doppler Ultrasound System for In Vivo Studies of Velocity Fields and Turbulent Stresses in Large Vessels," *Med Biol Eng Comput,* Vol. 32, pp. 55–62.

Nygaard, H., Paulsen, P. K., Hasenkam, J. M., Pedersen, E. M., and Rovsing, P. E., 1994b, "Turbulent Stresses Downstream of Three Mechanical Aortic Valve Prostheses in Human Beings," *J Thorac Cardiovasc Surg,* Vol. 107, pp. 438–446.

Shung, K. K., Cloutier, G., and Lim, C. C., 1992, "The Effects of Hematocrit, Shear Rate, and Turbulence on Ultrasonic Doppler Spectrum From Blood," *IEEE Trans Biomed Eng,* Vol. 39(5), pp. 462–469.

Shung, K. K., Yuan, Y. W., Fei, D. Y., and Tarbell, J. M., 1984, "Effect of Flow Disturbance on Ultrasonic Backscatter from Blood," *J Acoust Soc Am,* Vol. 75(4), pp. 1265–1272.

Strandness, D. E., Jr., 1990, "Duplex Scanning in Vascular Disorders," Raven Press, New York.

Talukder, N., Fulenwider, J. T., Mabon, R. F., and Giddens, D. P., 1986, "Poststenotic Flow Disturbance in the Dog Aorta as Measured with Pulsed Doppler Ultrasound," ASME J BIOMECH ENG, Vol. 108, pp. 259–265.

Taylor, K. J. W., Burns, P. N., and Wells, P. N. T., 1988, *Clinical Applications of Doppler Ultrasound,* Raven Press, New York.

Wells, P. N. T., 1994, "Ultrasonic Colour Flow Imaging," *Phys Med Biol,* Vol. 39, pp. 2113–2145.

Yongchareon, W. and Young, D. F., 1979, "Initiation of Turbulence in Models of Arterial Stenoses," *J Biomechanics,* Vol. 12, pp. 185–196.

Young, D. F., 1979, "Fluid Mechanics of Arterial Stenoses," ASME J BIOMECH ENG, Vol. 101(8), pp. 157–175.

Young, D. F., and Tsai, F. Y., 1973, "Flow Characteristics in Models of Arterial Stenoses - I. Steady Flow," *J Biomechanics,* Vol. 6(4-E), pp. 395–410.